Aerodynamic Effects of Oversized Tires and Modified Landing Gear on a Small Utility Airplane

L.S. Miller
G.G. Thumann
S.A. Sanborn
D.R. Ellis

National Institute for Aviation Research
Wichita State University
Wichita, KS 67260-0093

June 2000

Final Report

This document is available to the U.S. public
through the National Technical Information
Service (NTIS), Springfield, Virginia 22161.

U.S. Department of Transportation
Federal Aviation Administration

NOTICE

This document is disseminated under the sponsorship of the U.S. Department of Transportation in the interest of information exchange. The United States Government assumes no liability for the contents or use thereof. The United States Government does not endorse products or manufacturers. Trade or manufacturer's names appear herein solely because they are considered essential to the objective of this report.

1. Report No. DOT/FAA/AR-xx/xx	2. Government Accession No.	3. Recipient's Catalog No.	
4. Title and Subtitle AERODYNAMIC EFFECTS OF OVERSIZED TIRES AND MODIFIED LANDING GEAR ON A SMALL UTILITY AIRPLANE		5. Report Date June 2000	
		6. Performing Organization Code	
7. Author(s) L.S. Miller, G.G. Thumann, S.A. Sanborn, and D.R. Ellis		8. Performing Organization Report No. NIAR 2000-02	
9. Performing Organization Name and Address National Institute for Aviation Research Wichita State University 1845 N. Fairmount Wichita, KS 67260-0093		10. Work Unit No. (TRAIS)	
		11. Contract or Grant No. 96-G-011	
12. Sponsoring Agency Name and Address U.S. Department of Transportation Federal Aviation Administration Office of Aviation Research Washington, DC 20591		13. Type of Report and Period Covered Final Report	
		14. Sponsoring Agency Code	
15. Supplementary Notes .			

16. Abstract

An experimental investigation was conducted to identify the aerodynamic effects of oversized low-pressure (Tundra) tires and modified landing gear on a typical small utility airplane. Water tunnel and wind tunnel tests were performed using, respectively, a one-twentieth scale model and full-scale landing gear and tire components. Force and moment data show that oversized tires and taller landing gear cause a drag increase but do not substantially change basic static stability levels. A lack of directional stability for small sideslip angles observed in the water tunnel tests was not evident in wind tunnel tests done at a higher Reynolds number.

17. Key Words Tundra Tires Water Tunnel Testing Wind Tunnel Testing Longitudinal and Lateral Directional Static Stability Reynolds Number Effects		18. Distribution Statement This document is available to the public through the National Technical Information Service (NTIS), Springfield, Virginia 22161.	
19. Security Classif. (of this report) Unclassified	20. Security Classif. (of this page) Unclassified	21. No. of Pages	22. Price

Form DOT F1700.7 (8-72)   Reproduction of completed page authorized

TABLE OF CONTENTS

LIST OF FIGURES

LIST OF TABLES

NOMENCLATURE

Center of Gravity   CG
Wing Span   b
Wing Reference Chord   c
Wing Reference Area   S
Freestream Dynamic Pressure $q = 0.5 \rho V^2$
Freestream Flow Density ρ
Freestream Flow Speed   V
Reynolds Number $R = c \rho V /$
Freestream Flow Viscosity
Angle of Attack (Alpha)
Sideslip Angle (Beta)
Lift Force   L
Drag Force   D
Normal Force   N
Side Force   Y
Pitching Moment   PM
Rolling Moment   RM
Yawing Moment   YM
Normal Force Coefficient $C_N = N / [q \ S]$
Lift Coefficient $C_L = L / [q \ S]$
Drag Coefficient $C_D = D / [q \ S]$
Side Force Coefficient $C_Y = Y / [q \ S]$
Pitching Moment Coefficient $C_M = M / [q \ S \ c]$
Yawing Moment Coefficient $C_{YM} = YM / [q \ S \ c]$
Rolling Moment Coefficient $C_{RM} = RM / [q \ S \ c]$

EXECUTIVE SUMMARY

Because of concerns over frequent stall/spin accidents involving small utility aircraft equipped with oversize low-pressure ("Tundra") tires and modified landing gear, an experimental investigation was conducted to assess the effects of those non-standard features on the aerodynamics of an airplane typical of that class.

Water tunnel and wind tunnel tests were performed using, respectively, a one-twentieth scale Piper Super Cub model and full-scale Super Cub landing gear components.

Force and moment data show that oversize tires and taller or uncovered landing gear legs increase drag but do not substantially change basic levels of static stability.

Water tunnel results indicate directional instability for sideslip angles of 4° or less in high angle of attack flight; later wind tunnel tests with a one-seventh scale Super Cub model at higher Reynolds number (nearly 1,000,000 versus 16,000) show the directional stability to be positive under the same sideslip and angle of attack conditions.

1. INTRODUCTION

To facilitate operations from rough or soft unprepared fields, light utility aircraft are sometimes outfitted with oversized low-pressure tires (also known as "Tundra tires") and taller landing gear. The Piper Super Cub is one such airplane that commonly utilizes this modification, especially in Alaska. Unfortunately, there have been numerous incidents or accidents involving aircraft with larger tires and modified landing gear.

The exact reason for these accidents has not been fully defined. However, many reportedly occurred while the airplane was operating at low speeds (i.e., at high angles of attack) in turning flight. With this situation in mind, it has been hypothesized that the aerodynamic effects of the larger Tundra tire and gear have caused the plane to depart from controlled flight and crash. Specifically, it has been suggested that at high angles of attack and significant sideslip angles, the wake of the larger tires could be blanketing the empennage surfaces and adversely influencing the stability and control characteristics of the airplane.

1.1 GOAL OF THE INVESTIGATION

The goal of this investigation was to identify the incremental aerodynamic performance and stability effects of Tundra tires and other common modifications, including taller gear and removal of the gear covering. Particular emphasis was focused on the effects during high angle of attack and sideslip conditions.

2. INVESTIGATION METHODS

The experimental study utilized a combination of water and wind tunnel testing. A Piper Super Cub 1/20 scale model was constructed and installed in the Wichita State University (WSU) water tunnel for aerodynamic load and flow visualization measurements. Actual full-scale Super Cub landing gear and tire components were tested in the WSU 7 ft x 10 ft wind tunnel. Again load and flow visualization data were gathered. Results from these tests were used to assess the effects of tire and gear modifications on the aerodynamic characteristics.

2.1 WATER TUNNEL FEATURES

The WSU water tunnel has a test section with a 2 foot width, 3 foot height, and a length of about 5 feet. [1] This tunnel is capable of a maximum flow speed of about 1.0 ft/s, giving a Reynolds number of approximately 50,000 per foot of reference length. Most testing is performed at lower speeds, where the tunnel flow quality is high and best suited for conducting flow visualization observations. Transparent walls on four sides and a window downstream allow for viewing of the model and flow field during such testing.

The model was supported by a motor driven C-strut and sting assembly that allows positioning for angle of attack and yaw. The strut and sting minimize unfavorable aerodynamic interference effects, as compared to a multipoint strut mount. The tunnel flow speed was set and monitored manually during the tests to within approximately +/-0.02 ft/s. Prior to making detailed measurements, the tunnel anemometer system was calibrated.

2.1.1 WATER TUNNEL MODEL

Detailed information on the exact geometry of the Piper Super Cub was not readily available. Computer generated drawings were nonexistent, as might have been expected from the 1930s vintage of the basic design, as were true working drawings. A wide variety of published material, from various sources, was collected and used to make a reasonably accurate scale model. Shortcomings in the available information were supplemented by taking direct measurements from an actual Super Cub.

An "S-shaped" sting, of elliptical cross section, entered the plane through the aft lower fuselage and connected the balance, model, and C-strut together. The model utilized the standard fabric covered landing gear legs and could be run with standard, tundra, or no tires installed. Table 1 summarizes the important reference and geometrical constants. Figures 1A-1C show details of the model and its installation in the tunnel.

TABLE 1. WATER TUNNEL MODEL GEOMETRY AND REFERENCE VALUES

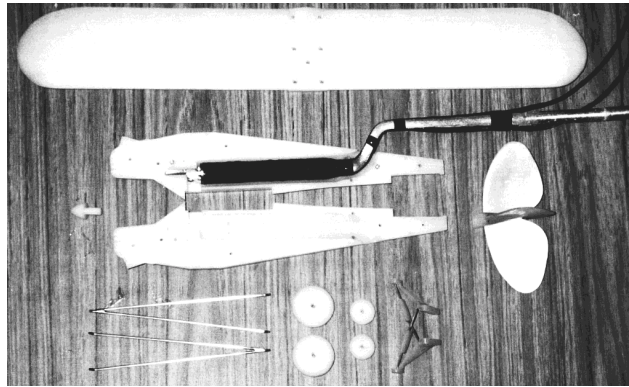| Scale	1/20
Wing Span (b)	21.125 in
Overall Length (l)	13.750 in
Reference Chord (c)	3.144 in
Wing Reference Area (S)	63.870 in

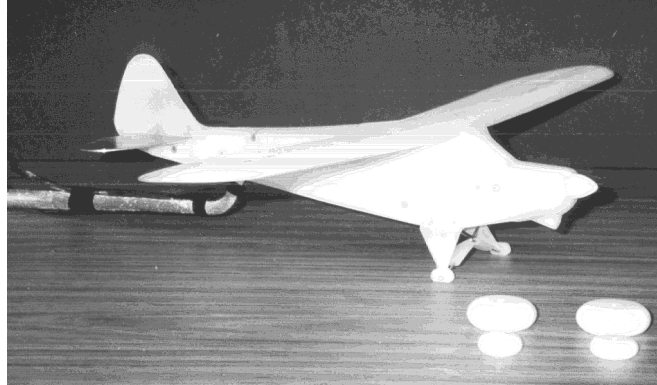FIGURE 1A. WATER TUNNEL MODEL ASSEMBLY, COMPONENTS, INTERNAL BALANCE, AND STING MOUNT

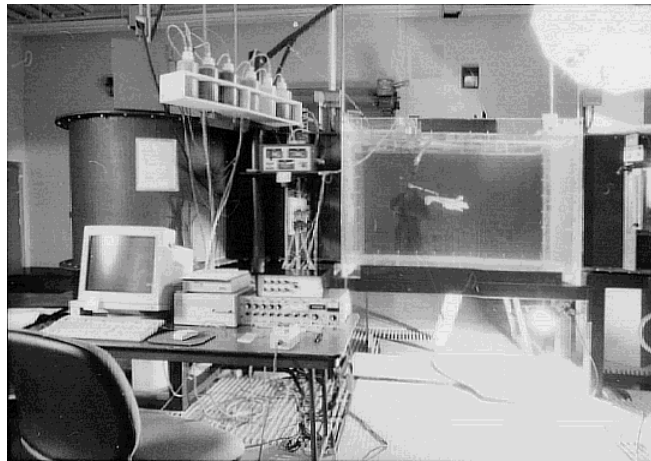FIGURE 1B. WATER TUNNEL MODEL ASSEMBLED, WITH STANDARD AND TUNDRA TIRES

FIGURE 1C. WATER TUNNEL, WITH MODEL INSTALLED, AND INSTRUMENTATION

2.1.2 WATER TUNNEL BALANCE AND DATA ACQUISITION

An internal balance was used to measure five components of the aerodynamic load acting on the model. Specifically, the model normal and side forces and pitching, rolling, and yawing moments were recorded. Drag was not measured since this degree of freedom was not available on the balance used.

The balance, all necessary signal conditioning equipment, and a computer-based data acquisition system were rented from Eidetics Corporation (the balance manufacturer). [2] Prior to testing, the balance was calibrated at Eidetics and check loads were again applied to verify accurate operation of the system after its installation in the WSU tunnel. Eidetics assisted with the balance assembly and check-out.

Static (i.e., model weight) tare measurements were performed for each model configuration and condition examined. These were subtracted from the test measurements so as to yield net aerodynamic data. Corrections for blockage (i.e., the presence of a model within an enclosed section) were not included in the data reduction process, since it was assumed that the small size

of the model relative to that of the tunnel should make these effects minimal. Moments were resolved about an assumed center of gravity (CG) location that was thirty percent (30%) aft of the wing leading edge and along the propeller thrust line.

Flow visualization was performed using the dye injection technique. Food coloring dye was delivered to the model via a hand-held wand or by small diameter (0.01 in) plastic tubes attached to the model exterior. The dye could be observed flowing about and downstream of the model.

2.1.3 WATER TUNNEL TEST CONDITIONS AND MATRIX

The water tunnel tests were conducted at a tunnel speed (V) of 0.73 ft/s or a dynamic pressure (q) of 0.522 lbs/ft^2. Based on the model reference chord (c) and freestream flow speed, this condition corresponds to a Reynolds number (R) of approximately 16,000. Angle of attack (α) excursions from -8   to + 18   and sideslip (β) excursions from 0   to + 20   were used for the tests.

2.2 WIND TUNNEL TESTS

Additional aerodynamic data were gathered using the WSU Walter H. Beech Memorial low-speed wind tunnel. [1] This facility is capable of producing test dynamic pressures up to 65 lb/ft^2 and has a test section that is 7-feet high and 10-feet wide. A six-component external balance measures model loads as a function of test conditions and model configuration. Data is collected, processed, and presented in real-time. Additional sensor data, including test section speed, atmospheric temperature and pressure, are also collected and recorded.

2.2.1 WIND TUNNEL MODEL

A partial configuration landing gear model, made from actual Super Cub components, was used in this part of the investigation. A rectangular platform, with rounded leading-and-trailing edges, was mounted to a steel pedestal that extended upward through the floor from the tunnel balance. This platform roughly simulates the lower surface of the airplane's fuselage and serves as a mounting location for the landing gear, with an effective angle of attack of 2.57 degrees. Figures 2A through 2C show photographs of the model (i.e., platform, gear, and tires) installed in the tunnel test section. As is illustrated, only the left-half side of the Cub gear was evaluated. A partial gear configuration was necessary to minimize tunnel flow blockage and aerodynamic interference effects.

FIGURE 2A. WIND TUNNEL MODEL; PLATFORM ONTO WHICH THE GEAR
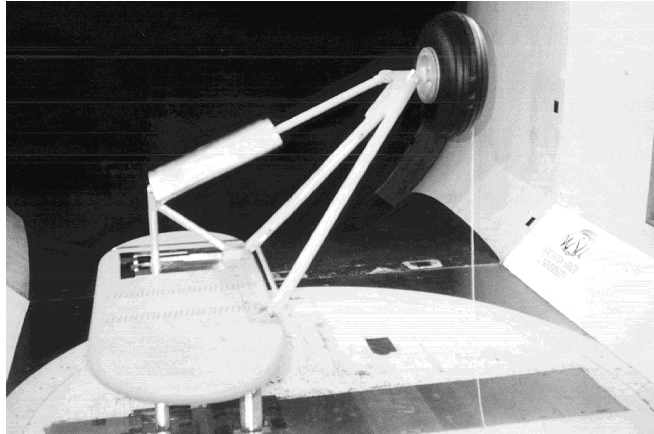ASSEMBLY ATTACHES (FRONT-QUARTER VIEW)

FIGURE 2B. WIND TUNNEL MODEL; INCLUDING GEAR ASSEMBLY AND
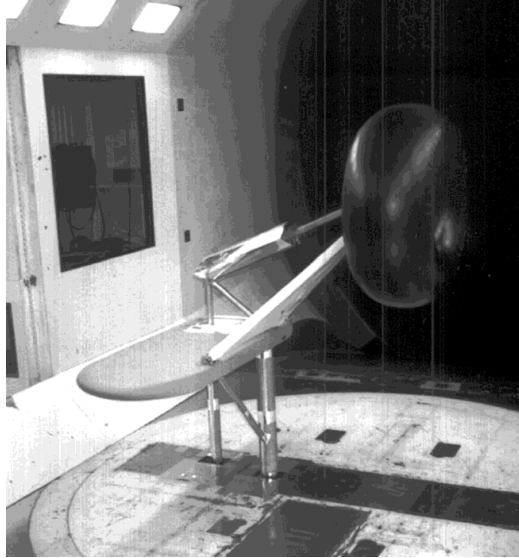STANDARD TIRE (AFT VIEW)

FIGURE 2C. WIND TUNNEL MODEL; INCLUDING GEAR ASSEMBLY AND TUNDRA
TIRE (AFT-QUARTER VIEW)

The wheel brake, bearing assembly, and landing gear shock-absorber and aerodynamic shroud
were also included on the model. Both a standard and larger size Tundra tire were evaluated,
along with standard and tall landing gear. In addition, the fabric covering was also removed
from each gear at one point in order to identify the effects of open gear on the aerodynamic
behavior. Model geometry and reference values are given in table 2.

TABLE 2. WIND TUNNEL MODEL GEOMETRY AND REFERENCE VALUES

Scale	Full	
Wing Span (b)	35.2 ft	
Reference Chord (c)	5.25 ft	
Wing Reference Area (S)	177.4 ft²	
Standard Tire Diameter	1.38 ft	(16.6 in)
Standard Tire Width	0.46 ft	(5.5 in)
Tundra Tire Diameter	2.58 ft	(31.0 in)
Tundra Tire Width	1.0 ft	(12.0 in)
Standard Landing Gear Length	2.50 ft	
Tall Landing Gear Length	2.83 ft	

2.2.2 WIND TUNNEL BALANCE AND DATA ACQUISITION

The standard underfloor wind tunnel force balance was used to measure drag and side force; lift
changes related to tire and gear configuration was assumed to be negligible. Corrections for
aerodynamic effects associated with testing in an enclosed environment, characteristic of a wind
tunnel as opposed to flight in a free atmosphere, were included in the data reduction.
Specifically, solid and wake blockage corrections were made using standard methods. [3,4] As
was the case for the water tunnel tests, moments were resolved about an assumed center of

gravity (CG) location (30% aft of the wing leading edge and along the propeller thrust line), for a virtual Super Cub airplane attached to the wind tunnel landing gear.

Simple flow visualization methods, utilizing a tuft-grid positioned downstream of the model and tufts attached to various parts of the landing gear and tires, were used to identify the tire/gear wake path and behavior.

3. RESULTS AND DISCUSSION

3.1 WATER TUNNEL TESTS

Figures 3 through 19 show the measured force and moment behavior as a function of tire size, gear installation, and flow angle (i.e., angle of attack or sideslip angle). Angle of attack sweeps for 0° and 20° of sideslip or sideslip sweeps for 0° and 12° angle of attack are presented. The 0° angle of attack correspond roughly to high speed flight situations and the 12° angle of attack to low speed.

Flow visualization testing showed that laminar flow separation was occurring over the wing upper surface for angles of attack greater than about 2.0 degrees. Traditional boundary layer trip and forced transition techniques were examined as a means for delaying flow separation and simulating higher Reynolds numbers (i.e., closer to full-scale). Unfortunately, these efforts were unsuccessful. Operation of the tunnel at maximum speed still prevented the development of a flow field that was representative of a full-scale aircraft. This early flow separation phenomenon is not unusual with unswept wings having relatively thick airfoil sections as used on the Super Cub, especially at very low Reynolds numbers. However, examination of the trends in the data is still useful.

In general, the data plots show the Tundra tire's impact to be relatively small when compared to the standard Super Cub tire behavior. Indeed, the two data sets typically coincide, with only minor differences in magnitude. Most importantly, the slopes of the pitching, rolling, and yawing moment coefficient curves typically parallel each other, suggesting minimal effect on static stability. Detailed results and brief related comments are provided in the following sections.

### 3.1.1 ZERO SIDESLIP, VARIABLE ANGLE OF ATTACK

Figures 3 through 7 show aerodynamic coefficient behavior for angle of attack changes at zero sideslip. The normal force (which is approximately the same as the lift force at these small angles of attack) is seen to be unchanged for any of the configurations tested. Figure 4, pitching moment coefficient versus angle of attack, shows that while the landing gear and tires cause a small nose-down pitching tendency, especially in the ±10 angle of attack range, the slopes of the curves do not change significantly with configuration, indicating no change in static longitudinal stability. Incremental effects of the Tundra tires are generally very small.

Side force and yawing moment coefficients are seen in figures 5 and 6 to remain near zero over the angle of attack range tested (note that the scales have been expanded to permit discrimination between configurations, and that the absolute values are very small).

Figure 7 shows a slight bias toward a left roll (negative RM) for angles of attack up to 14 , then a shift to a right rolling tendency at higher alpha values, along with more scatter in the data than for the other axes. The reasons for this are not known, but could be due to model asymmetry, flow angularity or flow unsteadiness; however, judging by the close grouping of data points at =0 and the near random behavior at other angles of attack, it appears that the gear and tire variations are not significant.
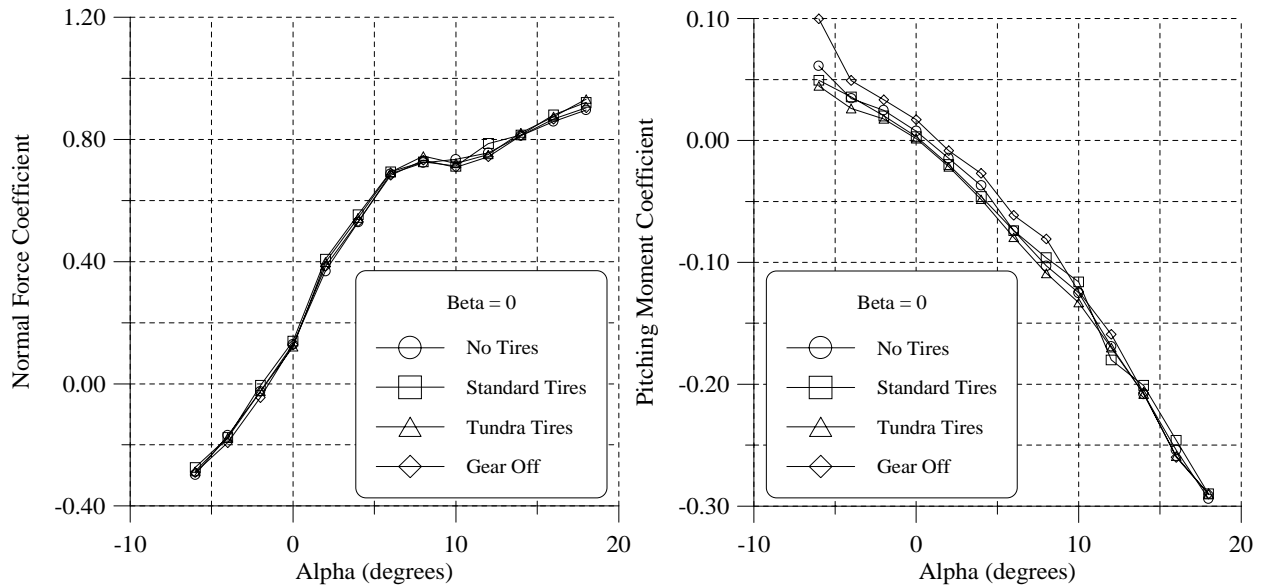
FIGURES 3 & 4. WATER TUNNEL DATA: TIRE EFFECTS ON NORMAL FORCE AND PITCHING MOMENT COEFFICIENTS AS A FUNCTION OF ANGLE OF ATTACK ( ), WITH 0   SIDESLIP ( )
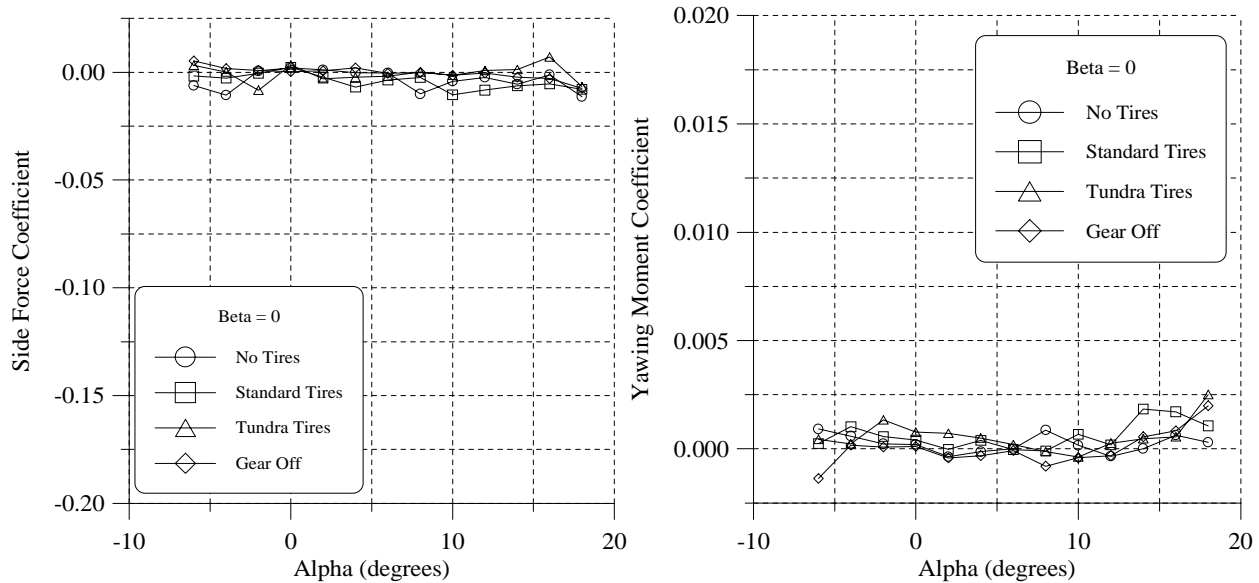
FIGURES 5 & 6. WATER TUNNEL DATA: TIRE EFFECTS ON SIDE FORCE AND
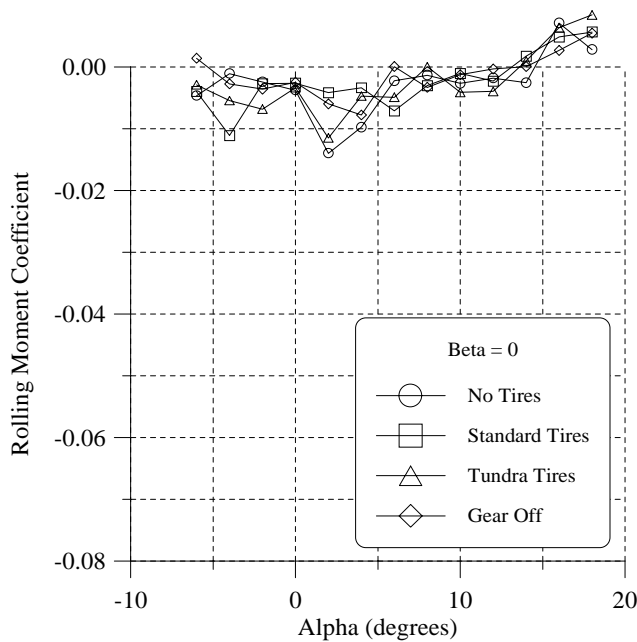YAWING MOMENT COEFFICIENTS AS A FUNCTION OF ANGLE OF ATTACK ( ),
WITH 0   SIDESLIP ( )

FIGURE 7. WATER TUNNEL DATA: TIRE EFFECTS ON ROLLING MOMENT
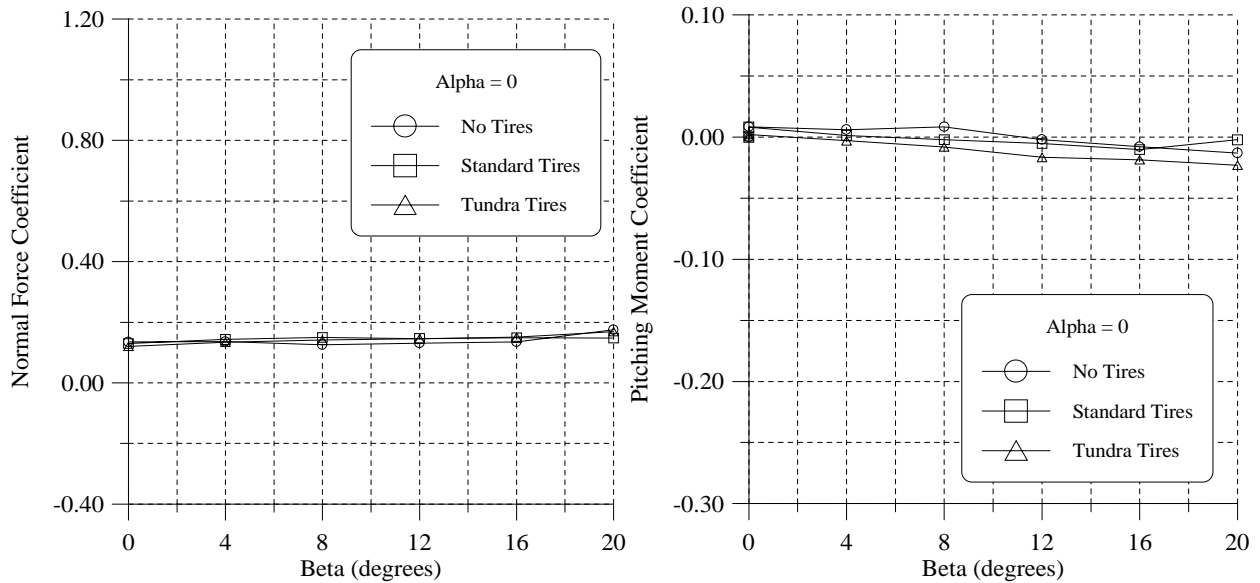COEFFICIENT AS A FUNCTION OF ANGLE OF ATTACK ( ),
WITH 0   SIDESLIP ( )

3.1.2 ZERO ANGLE OF ATTACK, VARIABLE SIDESLIP

Figures 8 and 9 identify the airplane's behavior at 0° angle of attack, or for relatively high
airspeed conditions. Figure 8 indicates that normal force does not change with sideslip, while

figure 9 shows a progressive nose down pitching moment change as tire size increases. This effect is small, however, and certainly trimmable in the actual airplane.

The Tundra tires cause an increase in side force, shown in figure 10, but the rate of change with sideslip remains unchanged. Figure 11 indicates that the directional stability, as measured by the slope of the yawing moment versus sideslip curve, is positive and essentially the same for standard or Tundra tires.

Figure 12, which is related to static lateral stability (dihedral effect) is less consistent, with the "no tires" and "Tundra tire" cases showing irregular behavior compared to the "standard tire." As in figure 7, there is an offset at $\beta = 0$ which might be due to model asymmetry or flow angularity. In general, though, the slopes are, on the average, negative (corresponding to positive static lateral stability) with no large differences due to the Tundra tires.

FIGURES 8 & 9. WATER TUNNEL DATA: TIRE EFFECTS ON NORMAL FORCE AND PITCHING MOMENT COEFFICIENTS AS A FUNCTION OF YAW ANGLE (β), AT 0 ANGLE OF ATTACK (α)

10
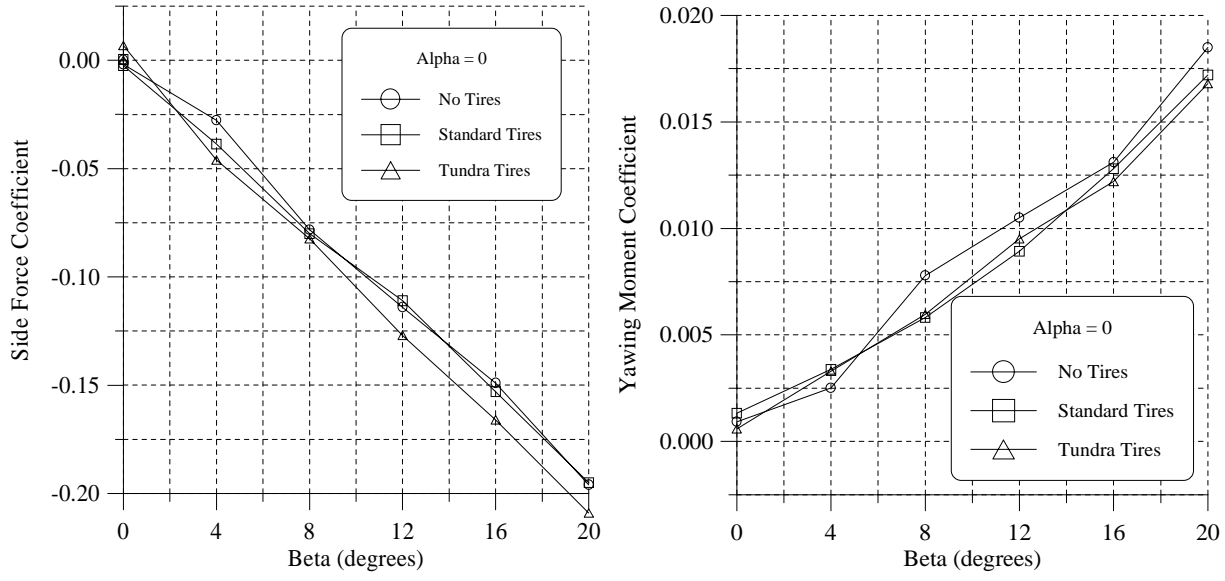
FIGURES 10 & 11. WATER TUNNEL DATA: TIRE EFFECTS ON SIDE FORCE AND
YAWING MOMENT COEFFICIENTS AS A FUNCTION OF SIDESLIP ANGLE (   ),
AT 0   ANGLE OF ATTACK (   )
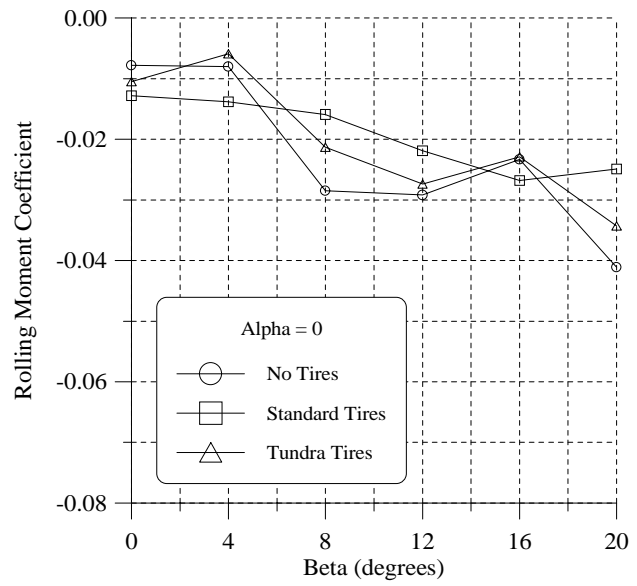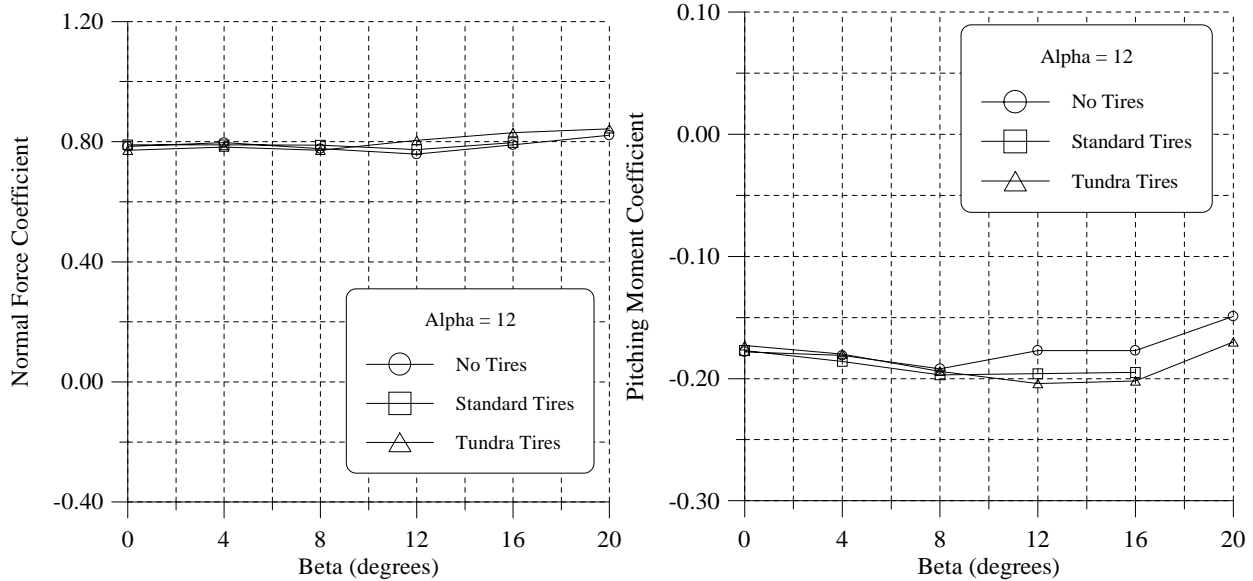

FIGURE 12. WATER TUNNEL DATA: TIRE EFFECTS ON ROLLING MOMENT
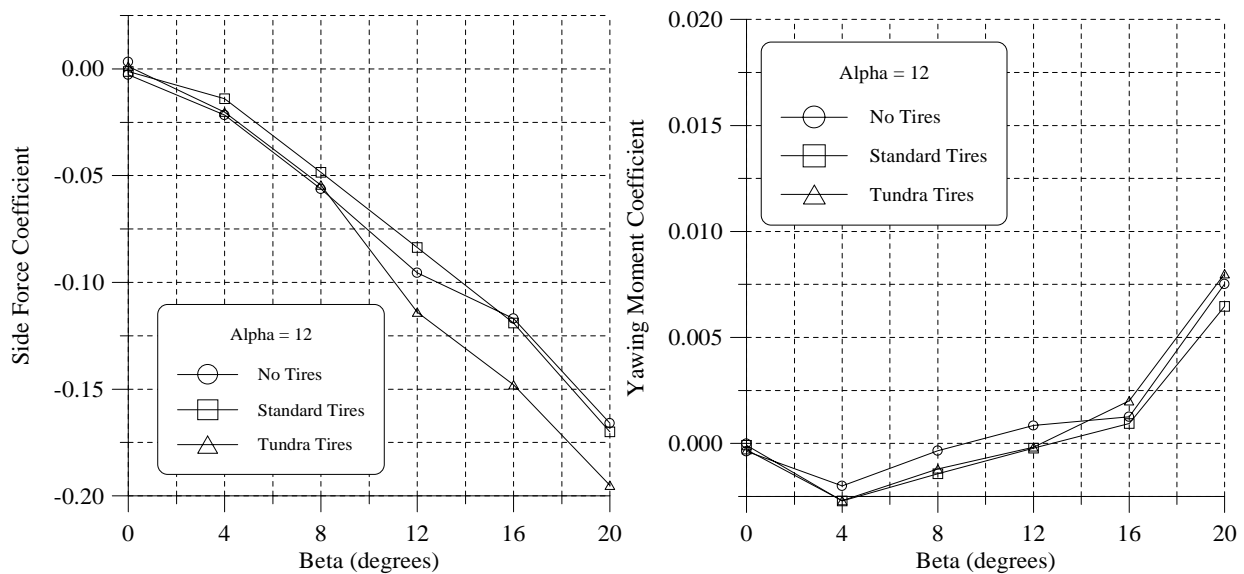COEFFICIENT AS A FUNCTION OF SIDESLIP ANGLE (   ),
AT 0   ANGLE OF ATTACK (   )

3.1.3 HIGH ANGLE OF ATTACK, VARIABLE SIDESLIP

Figures 13 through 17 illustrate results that are characteristic of the airplane flying at a high
angle of attack or at low speeds, perhaps near stall. In most cases, only minor magnitude
changes in the aerodynamic coefficients are observed due to the Tundra tires.

Figure 16 is significant in that it shows that the airplane in this high angle of attack setting is directionally unstable out to a sideslip angle of 4 , regardless of tire configuration. Beyond this sideslip angle, the stability becomes positive and a trim point is reached at beta = 12   with tires on. This unstable region is most likely due to a blanketing of the vertical tail by the separated wake from the forward portions of the model at this high angle of attack and small sideslip angle. At higher sideslip angles the vertical tail apparently moves out of the wake and regains its effectiveness.

FIGURES 13 & 14. WATER TUNNEL DATA: TIRE EFFECTS ON NORMAL FORCE AND PITCHING MOMENT COEFFICIENTS AS A FUNCTION OF SIDESLIP ANGLE ( ), AT 12   ANGLE OF ATTACK ( )

FIGURES 15 & 16. WATER TUNNEL DATA: TIRE EFFECTS ON SIDE FORCE AND YAWING MOMENT COEFFICIENTS AS A FUNCTION OF SIDESLIP ANGLE ( ), AT 12   ANGLE OF ATTACK ( )
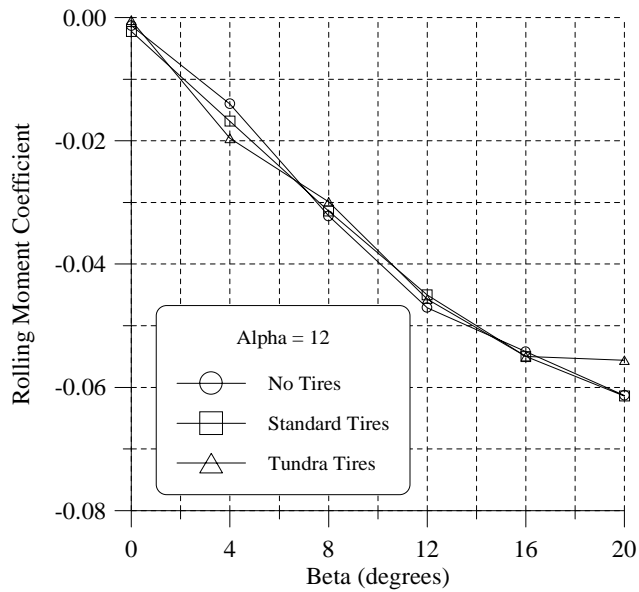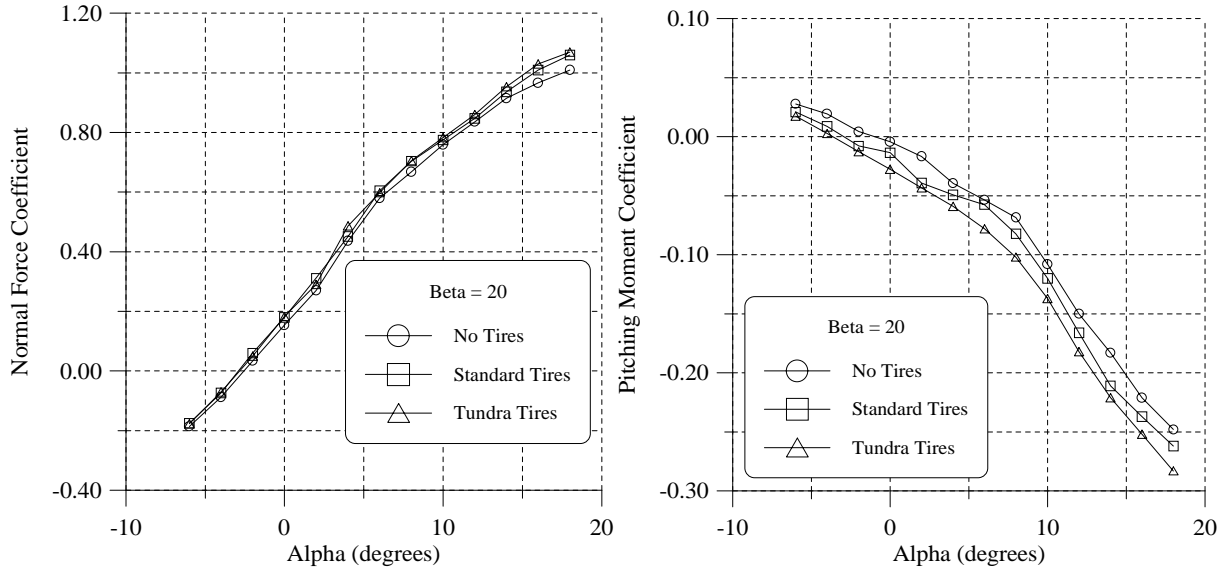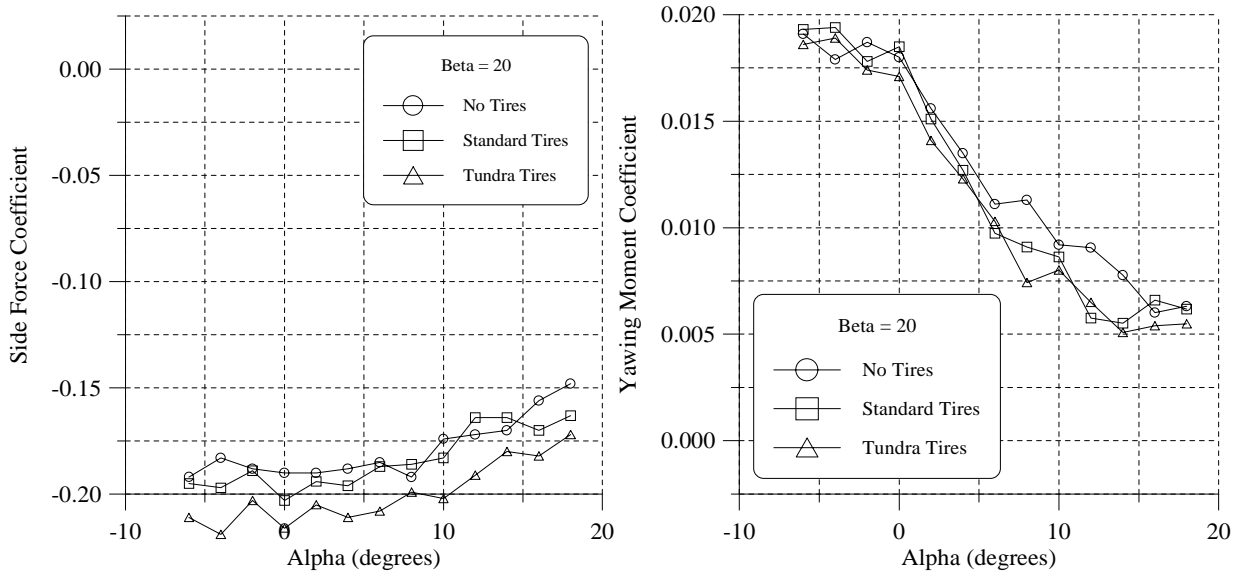
12

FIGURE 17. WATER TUNNEL DATA: TIRE EFFECTS ON ROLLING MOMENT
COEFFICIENT AS A FUNCTION OF SIDESLIP ANGLE ( ),
AT 12 ANGLE OF ATTACK ( )

3.1.4 HIGH SIDESLIP, VARIABLE ANGLE OF ATTACK

Figures 18 through 22 are for a sideslip angle of 20°, perhaps representative of an extreme
crosswind or unusual flight condition. Again, normal force and pitching moment are well-
behaved, and though there is scatter in the data (probably due to separated flow at this high
sideslip angle), there are no serious anomalies due to tire size.

FIGURES 18 & 19. WATER TUNNEL DATA: TIRE EFFECTS ON NORMAL FORCE AND
PITCHING MOMENT COEFFICIENTS AS A FUNCTION OF ANGLE OF
ATTACK (   ), AT 20   SIDELSIP (   )

FIGURES 20 & 21. WATER TUNNEL DATA: TIRE EFFECTS ON SIDE FORCE AND
YAWING MOMENT COEFFICIENTS AS A FUNCTION OF ANGLE OF ATTACK (   ),
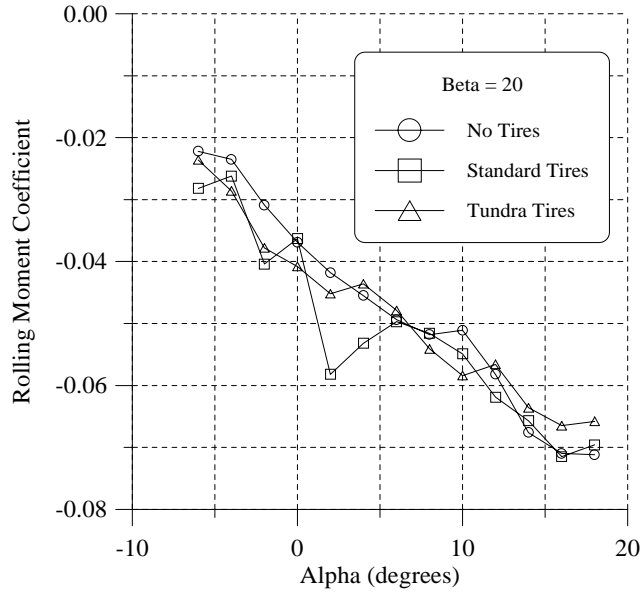AT 20   SIDESLIP (   )

14

FIGURE 22. WATER TUNNEL DATA: TIRE EFFECTS ON ROLLING MOMENT
COEFFICIENT AS A FUNCTION OF ANGLE OF ATTACK ( ), AT 20   SIDESLIP ( )

3.2 WIND TUNNEL TESTS

Figures 23 through 32 show the measured force and moment behavior of the wind tunnel landing
gear model as a function of sideslip angle. In all cases the effective angle of attack was constant
and equal to 2.57 degrees. Tall gear and no-fabric covering configurations were also examined
during this part of the investigation. Data shown in these figures are for a dynamic pressure of
30.00 lb/ft^2 or a Reynolds number of 5,200,000.

The observed pitching moment coefficient change due to the use of the Tundra tire (shown in
figure 23) is notably less than that seen in the water tunnel tests (figure 4). This result suggests
that the water tunnel data may be affected significantly by Reynolds number and that the larger
tire's impact was over-predicted. The other aerodynamic coefficients are influenced by the
Tundra tire in the same way as observed in the water tunnel. Figure 27 shows an approximate
30-count (0.0030) drag coefficient penalty for Tundra tire use.

Landing gear height and covering effects are shown in figures 28 through 32 (in each case the
standard Super Cub tire was used). According to figure 31, gear height apparently influences
side force more than covering. Figure 32 illustrates that removal of the gear covering or a
change to tall gear creates higher drag (approximately ten counts). For much of the range, the
tall covered gear yielded the same drag as the standard uncovered gear.
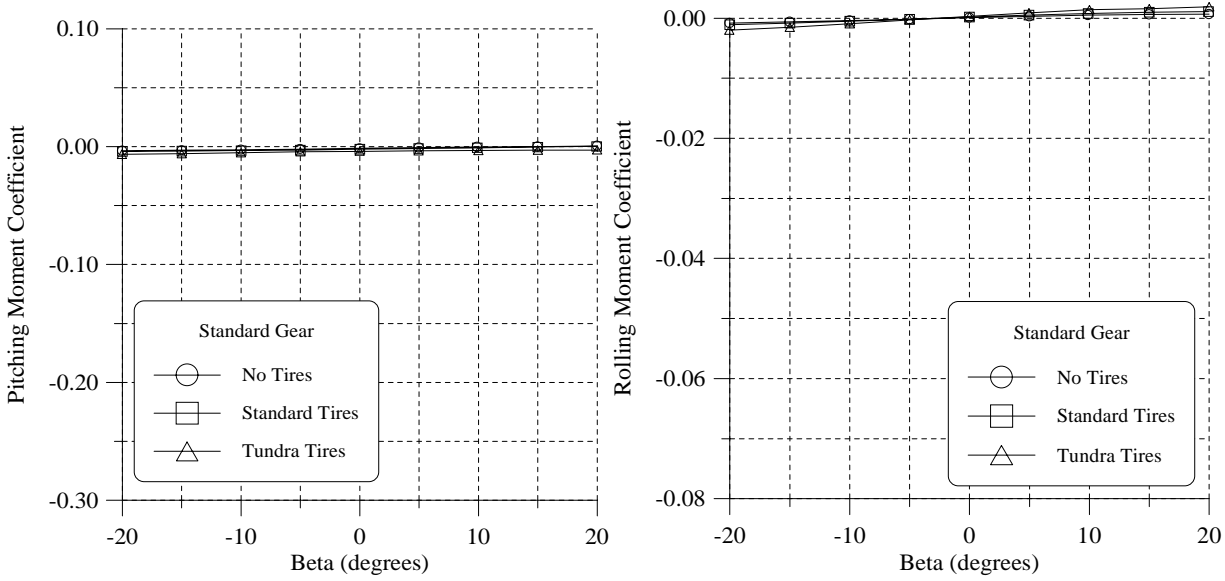
FIGURES 23 & 24. WIND TUNNEL DATA: TIRE EFFECTS ON PITCHING AND
ROLLING MOMENT COEFFICIENTS AS A FUNCTION OF SIDESLIP ANGLE (   ),
AT 2.57   ANGLE OF ATTACK (   )

FIGURE 25. WIND TUNNEL DATA: TIRE EFFECTS ON YAWING MOMENT
COEFFICIENT AS A FUNCTION OF SIDESLIP ANGLE (   ),
AT 2.57   ANGLE OF ATTACK (   )

16

FIGURES 26 & 27. WIND TUNNEL DATA: TIRE EFFECTS ON SIDE AND DRAG FORCE
COEFFICIENTS AS A FUNCTION OF SIDESLIP ANGLE (   ),
AT 2.57   ANGLE OF ATTACK (   )

FIGURES 28 & 29. WIND TUNNEL DATA: GEAR EFFECTS ON PITCHING AND
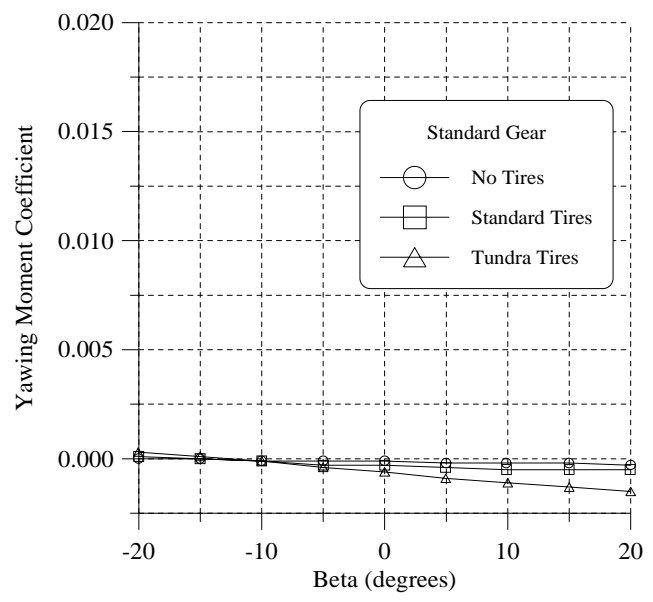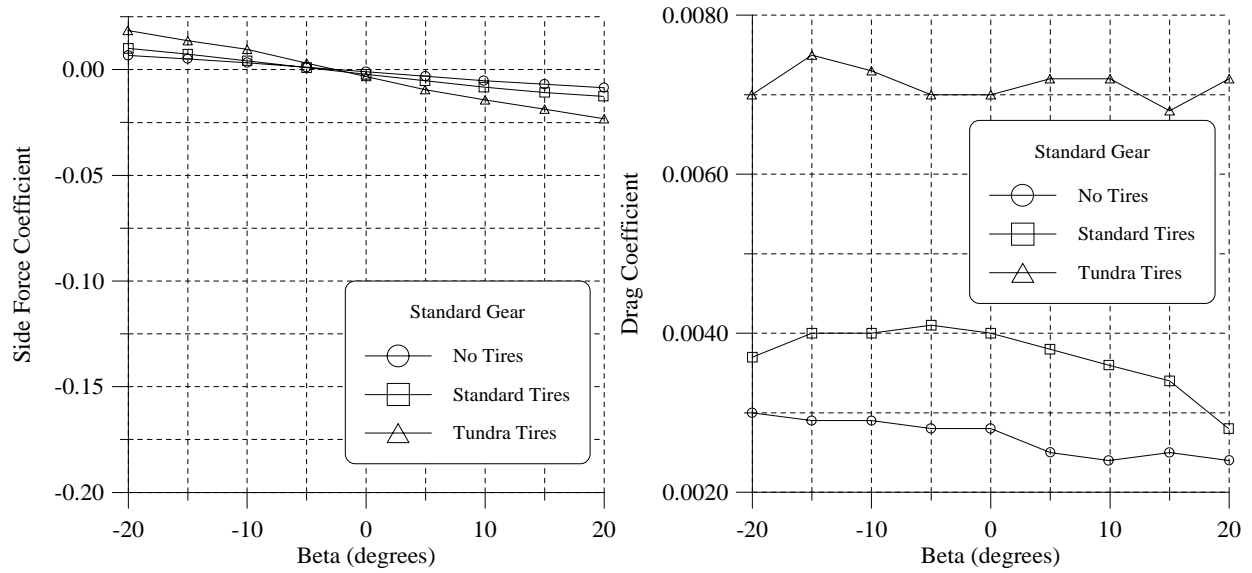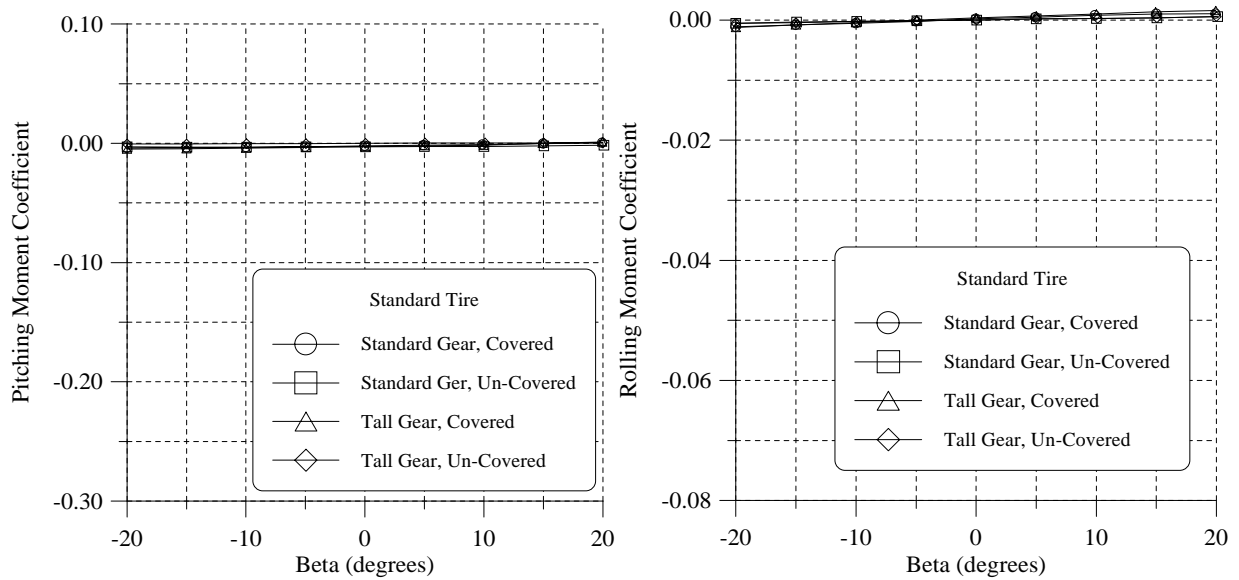ROLLING MOMENT COEFFICIENTS AS A FUNCTION OF SIDESLIP ANGLE (   ),
AT 2.57   ANGLE OF ATTACK (   )

FIGURE 30. WIND TUNNEL DATA: GEAR EFFECTS ON YAWING MOMENT
COEFFICIENT AS A FUNCTION OF SIDESLIP ANGLE (   ),
AT 2.57   ANGLE OF ATTACK (   )

FIGURE 31. WIND TUNNEL DATA: GEAR EFFECTS ON SIDE FORCE COEFFICIENT
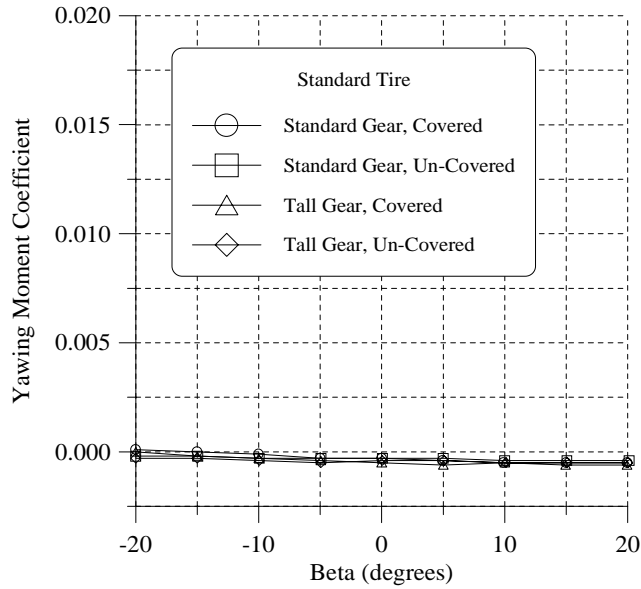AS A FUNCTION OF SIDESLIP ANGLE (   ), AT A 2.57   ANGLE OF ATTACK (   )
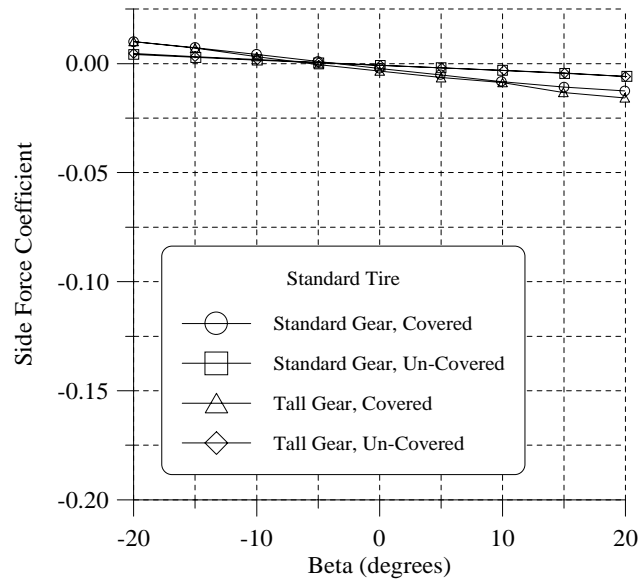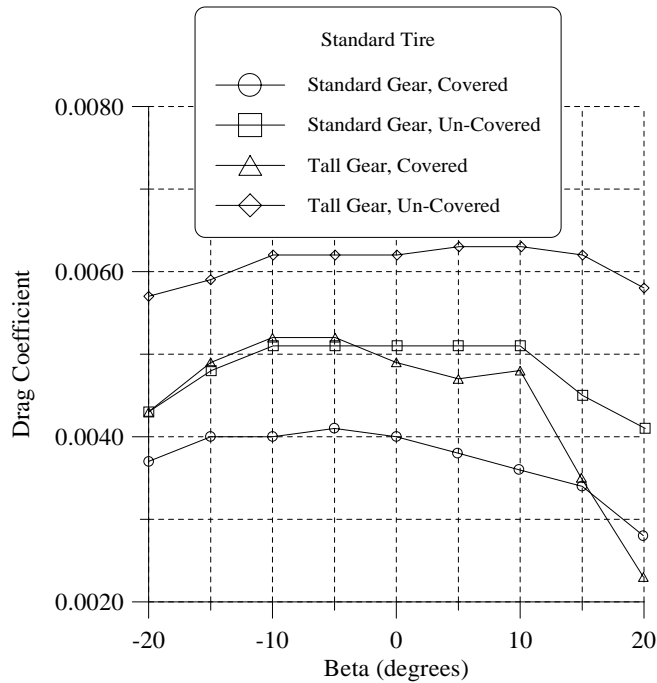
FIGURE 32. WIND TUNNEL DATA: GEAR EFFECTS ON DRAG FORCE COEFFICIENT AS A FUNCTION OF SIDESLIP ANGLE ( ) AT A 2.57   ANGLE OF ATTACK ( )

3.3 FLOW VISUALIZATION

Flow visualization was employed during both the water and wind tunnel tests. The flow moving from around the gear and tires was observed to move downstream and at high angles of attack and sideslip, to impinge on the tail surfaces. The wake flow was typically turbulent and unsteady, and may have been a factor in the directional instability observed in figure 16.

3.4 REYNOLDS NUMBER EFFECTS

The water and wind tunnel data were collected at notably different Reynolds numbers (16,000 verses 2,100,000 to 7,000,000). As noted in Section 3.1, water tunnel flow visualization experiments indicated that the flow over the wing was separated except at angles of attack smaller than about 2 , because of the low Reynolds number. This situation has the potential to affect the accuracy of the water tunnel data, most notably the magnitude of the normal force and yawing moment coefficients, the later most likely due to wake interference with the vertical tail.

A recent thesis investigation (not a part of this grant) addressed differences between results obtained at various Reynolds numbers from 16,000 to 7,000,000. [5] One-seventh scale Piper Super Cub model tests were carried out in the WSU low speed wind tunnel at Reynolds numbers of 430,000 and 1,000,000. Results were compared to this investigation's water and (partial-model) wind tunnel data and showed that the water tunnel longitudinal, lateral, and directional static stability behavior were adequately measured and that only the magnitudes of forces and moments differed significantly. The exception was the directional stability at high angle of attack; the water tunnel test indicated that the airplane was unstable for angles of sideslip smaller

than 4° (see figure 16 and the accompanying description in Section 3.1.3), whereas the wind tunnel data for a Reynolds number of nearly 1,000,000 show positive stability. A comparison of these results is given in the Addendum, Section 6.

4. CONCLUSIONS

Water and wind tunnel experiments were performed to identify the aerodynamic and performance effects of larger diameter (Tundra) tires and modified landing gear on a Piper Super Cub. On the basis of the investigation results, the following conclusions are offered:

1. Water tunnel data indicate that the airplane's basic longitudinal, lateral, and directional static stability behavior does not change significantly as a result of using Tundra tires or taller gear.

2. Drag and side force coefficients were notably affected by tire size and gear configuration. A thirty-count (0.0030) drag coefficient increase was observed as a result of using Tundra tires. Removal of the covering or lengthening the gear increases the drag by approximately ten-counts for each change. Gear height appears to have a more significant impact on side force than does gear covering.

3. Flow visualization showed landing gear wake impingement on the airplane tail surfaces, but specific performance, controllability, or stability effects could not be linked to the flow behavior.

4. The water tunnel model's aerodynamic behavior was subject to Reynolds number effects. Specifically, laminar flow separation occurred over the entire wing for angles of attack above 2.0 degrees, affecting the magnitude of the normal force measurement and causing an apparent directional instability for sideslip angles smaller than 4° when operating at high angles of attack. Subsequent wind tunnel testing at higher Reynolds number (1,000,000 versus 16,000 for the water tunnel) showed the model to be stable for those conditions.

5. Control surface (i.e., elevator, rudder, and aileron) effectiveness was not evaluated in this investigation. Further testing, with a more sophisticated model, would be necessary to determine whether or not control power is adversely affected by the wake flow from the larger tires.

5. REFERENCES

1. Johnson, B.L., "Facility Description of the Walter H. Beech Memorial 7 X 10 Foot Low-Speed Wind Tunnel," AR93-1, Aerodynamic Laboratories, Wichita State University, Wichita, Kansas, 67260-0093.

2. Suarez, C.J., <u>Five-Component Balance for Water Tunnel Applications,</u> Eidetics Corporation, Torrance, California.

3. Rae, W.H. and Pope, A., <u>Low-Speed Wind Tunnel Testing,</u> Second Edition, John Wiley & Sons, New York, 1984.

4. Johnson, B.L., Leigh, J.E. and Moore, K.A., "Three-Dimensional Force Data Acquisition and Boundary Corrections for the Walter Beech Memorial 7 X 10 Foot Low-Speed Wind Tunnel," AR93-2, Aerodynamic Laboratories, Wichita State University, Wichita, Kansas, 67260-0093.

5. Thumann, G.G., "An Assessment of Water Tunnels for Aerodynamic Performance Evaluation of a General Aviation Aircraft," Thesis, Wichita State University, Wichita, Kansas, 67260-0093, Fall 1997.

6. ADDENDUM

6.1 DIRECTIONAL STABILITY COMPARISON

Water tunnel data (see figure 16) indicate that the airplane with either standard or Tundra tires is directionally unstable (i.e., negative slope of C_{RM} versus β) for angles of sideslip less than 4° when flown at a high angle of attack ($\alpha=12°$). The discussion in Section 3.1.3 suggests that this is due to the vertical tail being in the separated flow from the wing and forward fuselage noted in the flow visualization tests.

Wind tunnel testing done later with a much larger (1/7 versus 1/20 scale) model and at higher Reynolds number (nearly 1,000,000 versus 16,000) shows no evidence of static instability, though the level of stability is lower for sideslip angles under 4° than for larger angles. [5] This is evident in figure A1 which shows data from both water tunnel and wind tunnel tests.

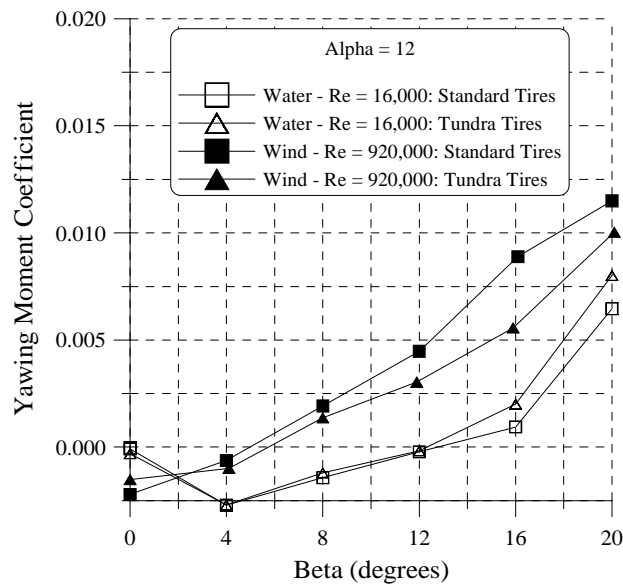FIGURE A1. COMPARISON OF YAWING MOMENT COEFFICIENT AS A FUNCTION OF SIDESLIP ANGLE (β) FROM WATER TUNNEL AND WIND TUNNEL TESTS

22